Steering between Level Repulsion and Attraction: Beyond Single-Tone Driven Cavity Magnon-Polaritons

Isabella Boventer

Institute of Physics, Johannes Gutenberg University Mainz, 55128 Mainz, Germany Unité Mixte de Physique CNRS, Thales, University Paris-Sud, Université Paris-Saclay, 91767 Palaiseau, France

Mathias Kläui

Institute of Physics, Johannes Gutenberg University Mainz, 55099 Mainz, Germany Graduate School of Excellen Materials Science in Mainz, Staudinger Weg 7, 55128 Mainz, Germany

Rair Macêdo

James Watt School of Engineering, Electronics & Nanoscale Engineering Division, University of Glasgow, Glasgow G12 8QQ, United Kingdom

Martin Weides

James Watt School of Engineering, Electronics & Nanoscale Engineering Division, University of Glasgow, Glasgow G12 8QQ, United Kingdom

E-mail: Martin.Weides@glasgow.ac.uk

Abstract. Cavity-magnon polaritons (CMPs) are the associated quasiparticles of a hybridization between cavity photons and magnons in a magnetic sample placed in a microwave resonator. In the strong coupling regime, where the macroscopic coupling strength exceeds the individual dissipation, there is a coherent exchange of information. This renders CMPs as promising candidates for future applications such as in information processing. Recent progress on the study of the CMP allows now not only to obtain CMPs, but also to tune the coupling strength such as enhancing or suppressing the information exchange. Here, we go beyond standard single-tone driven CMPs and employ a two-tone driven CMP. We control the coupling strength by the relative phase ϕ and amplitude field ratio δ_0 between both tones. Specifically, we derive a new expression from Input-Output theory for the study of the two-tone driven CMP and discuss the implications on the coupling strength. Furthermore, we examine intermediate cases where the coupling strength is tuned between its maximal and minimal value and, in particular, the high δ_0 regime.

Steering between Level Repulsion and Attraction: Beyond Single-Tone Driven Cavity Magnon-Polaritons2 netic resonance, Hybrid systems, Strong coupling.

1. Introduction

The phenomenon of a (strong) coupling of magnons, the associated quanta of collective spin wave excitations to microwave cavity photons resulting in cavity magnon-polaritons (CMPs) has been the subject of numerous works in the past few years [1–9]. The ability to couple magnons to different physical systems, through magneto-optical [10– 12 to optical or by magnetostrictive interaction to mechanical [13] and cavity photons simultaneously makes CMPs highly interesting for various applications [8]. For instance, it allows for a bidirectional conversion of microwaves to optical light [14], or coupling magnons with superconducting circuits, i.e. qubits [15]. The context of these studies varies from purely classical [10, 14, 16–18] to quantum based approaches [15, 19]. For a strongly coupled cavity-magnon system where the coupling strength exceeds the individual dissipation from each subsystem at resonance, that is $\omega_c = \omega_m \equiv \omega_c$, the cavity photon and magnon states hybridize. As a result of the simultaneous coupling of N contributing spins of the magnonic sample, one observes the opening of a frequency gap $\Delta\omega = 2g_{\rm eff} = 2g_0\sqrt{N}$ due to level repulsion [4]. Here, g_0 denotes the single spin and g_{eff} denotes the effective macroscopic coupling strength in the dispersion spectrum. The observation of such an avoided crossing (anti-crossing) is a characteristic feature of cavity magnon-polaritons (CMPs) and it enables the study of properties of said systems [7].

In most of these works however, being able to control the coupling constant is imperative; whether the ultimate goal is to achieve stronger coupling or to control the actual state of coupling [20]. While most of the above mentioned initial studies have concentrated in the case of level repulsion which leads to said avoided level crossing – also known as Rabi splitting [21] – more recently, another phenomenon has emerged called level attraction [22–26]. In order to achieve this, several approaches have been employed so far. The most simplistic one, perhaps, is moving the magnetic sample to different positions within the 3-dimensional microwave resonator [24] or even a 2-dimensional one [27]. In most of these experiments, however, a microwave signal from an external source was coupled into the resonator and thereby directly driving the cavity photons at a certain cavity resonance frequency ω_c . In such setups, a magnetic sample was placed into an antinode of the time varying magnetic field from the chosen cavity resonator mode resulting from alternating currents (AC). These AC fields would then drive ferromagnetic resonances in the magnetic sample, i.e. it would excite magnons resonating at a frequency ω_m [1].

In a recent work, we have shown a way to access the regime of level attraction by the addition of a second external microwave input and by externally controlling the relative phase ϕ and amplitude ratio δ_0 of the AC magnetic fields within the resonator [28]. By tuning the relative phase to $\phi = \pi$ and setting $\delta_0 = 1$, we observed a full closure of the anticrossing gap which we also call level merging. If the phase is kept fixed and $\delta_0 > 1$, we enter the regime of level attraction. In this work, we present details of the conditions under which this coupling might happen, study intermediate phases where level repulsion and attraction are both present and the impacts of higher

 δ_0 on our system. We focus on the coupling of cavity photons to magnons in the Kittel mode, which is a special instance of a magnetostatic mode with wavevector $\mathbf{k} = 0$. The Kittel mode denotes the uniform precession for all spins and has a dispersion $\omega_m = \gamma \mathbf{H}_0$, where γ is the gyromagnetic ratio and \mathbf{H}_0 is a static magnetic field externally applied [29]. As it typically shows the highest coupling strength to the cavity photons, numerous experiments studied CMPs via the coupling to the Kittel mode [2, 4, 5, 30].

The experimental setup is described in Sec. 2, followed by the theory detailed in Sec. 3 and the experimental results and discussions are given in Sec. 4.

2. Experimental Setup

Up until now, there have been several different and well established methods to probe the coupling between cavity and magnons experimentally where one of the most common ones is microwave spectroscopy. In this, the system's transmission or (and) reflection parameters are recorded [30]. Another method is that of electrical detection employing a voltage generated from a combination from spin pumping and the inverse spin Hall effect [31, 32]. Brillouin light scattering spectroscopy has also been recently used to achieve the same goal [33].

For our two-tone driven CMP experiment, we employed microwave resonator spectroscopy and modified a previous single tone driven setup [28, 34]. experimental setup, we employ a reentrant cavity resonator with resonance frequency $\omega_c/2\pi = 6.5 \,\mathrm{GHz}$ and insert a commercially bought sphere $(d = 0.2 \,\mathrm{mm}, [35])$ made of Yttrium-Iron-Garnet (YIG) into the antinode of the resonator's AC magnetic field [3, 34]. Accordingly, Fig. 1 gives a detailed overview of the position of the two microwave inputs [topview, a.)], the relative orientation of the single winded metallic loop which constitutes the second input, called magnon port, in combination with the AC magnetic fields at the sample's position [b.) and the complete experimental apparatus [c.). The Vector Network Analyzer (VNA) serves as the single microwave source of the system as illustrated in Fig. 1. It is split using a power divider into two signal paths. As can be inferred from Fig. 1 b.), the magnon port is tilted by 45° to the cavity resonator's xy-plane. We found experimentally, that this angle gives the best compromise between minimal crosstalk and spatial limitations of our experimental setup. The non-zero angle out of the xy-plane results in two AC magnetic field components (red), i.e. $h_{z,AC}^{magnon}$ and $h_{x,AC}^{magnon}$. There, $h_{z,AC}^{magnon}$, is parallel to the direction of the external, static magnetic field $\mathbf{H}_{\text{ext}} = (0, 0, H_{\text{ext}})$ and, hence, does not drive the magnons. However, $h_{\text{x,AC}}^{magnon}$ is orientated such that it also drives ferromagnetic resonance but does not directly couple to the cavity photon field (blue) because $h_{\rm x,AC}^{magnon} \perp h_{\rm AC}^{cavity}$. Thus, both inputs can be considered to act independently on the magnons, once indirectly by the first input, also called cavity port, via the coupling at resonance and directly by the second input, i.e. the magnon port. Experimentally, there is a suppressed but non-zero residual direct coupling to the cavity photons by a small component parallel to h_{AC}^{cavity} . This crosstalk may be, for instance, caused by another small tilt of the coupling loop along the xz-

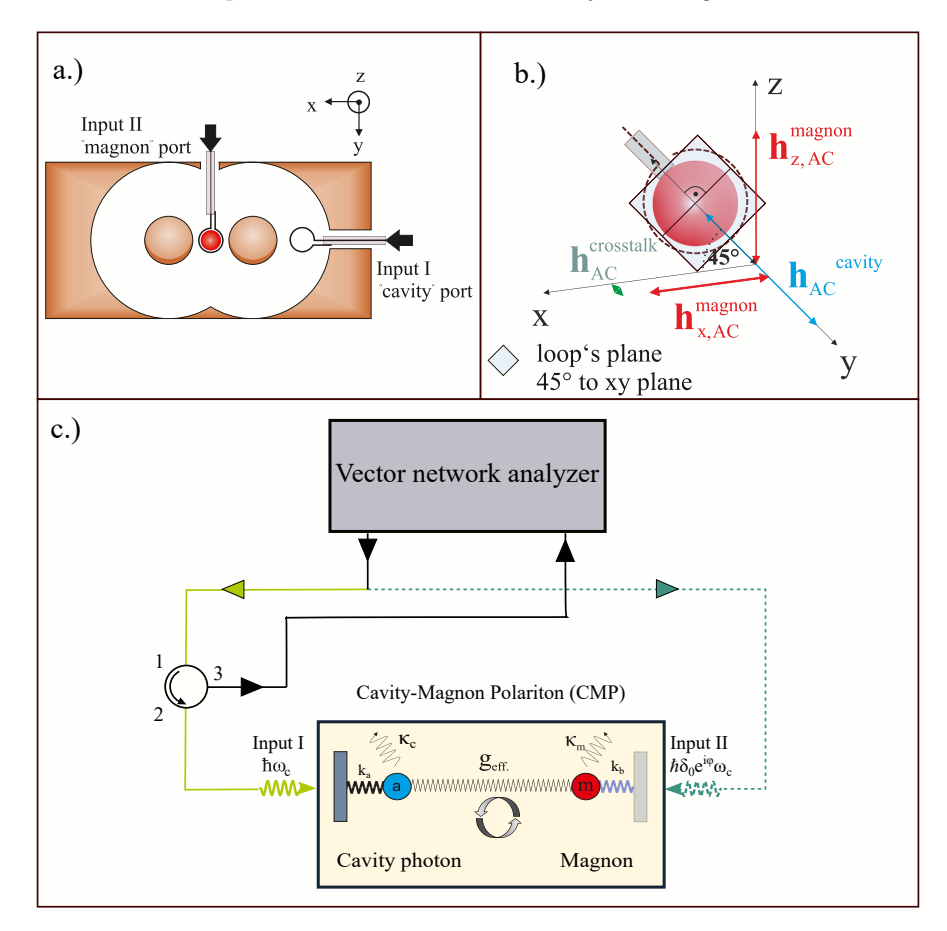


Fig. 1. Overview over the implementation of the two tones for the coupling strength control of the CMP. a.) Position of both inputs, where the microwave signal is inductively coupled by a single winded metallic loop into the cavity resonator. b.) Relative orientation of the magnon port's coupling loop around an sphere made of Yttrium-Iron-Garnet (YIG) and alignment of the intracavity AC magnetic fields. c.) Schematics of the experimental setup for a single tone driven (solid lines) and a two-tone driven (dotted green line) CMPs measurement in reflection from the cavity port. The CMP is illustrated as a system of two harmonic oscillators coupled by spring. Here this represents the effective coupling strength. Whilst the spring constants k_a and k_b give the coupling efficiency to the microwave feedline, the internal losses from each constituent are given by κ_c and κ_m

plane. Specifically, in the experiment, we measure at the cavity port and record the reflection parameter $S_{11}(\omega)$ at the second port of a vector network analyzer (c.f. Fig. 1 c.)). There, we sketch the experimental setup for both a single tone CMP measured in reflection mode at the cavity port (the dashed parts are then not to be included) and a two-tone driven CMP. The latter is depicted by the green dotted line.

In Fig. 1 c.), we illustrate the CMP by a system of two coupled harmonic oscillators with individual loss parameters κ_c for the cavity photons and κ_m for the magnons and corresponding coupling losses due to the coupling to the external microwave feedline (c.f. Ref.[7]). Now, such an introduction of a second input in the experimental setup for the study of the CMP, requires the modification of the standard reflection parameter

Steering between Level Repulsion and Attraction: Beyond Single-Tone Driven Cavity Magnon-Polaritons6 $S_{11}(\omega)$. This is discussed in the next section.

3. Theoretical Background

Here, we derive an expression to model a two-tone cavity magnon-polariton spectroscopic experiment measured in reflection. However, in order to show clearly the implications of a second input, we find it necessary to introduce the concepts and main assumptions for the study of a simple single tone driven CMP first.

3.1. Spectroscopy with one tone

An experimental setup such as the one shown in Fig. 1 c.) – ignoring the dotted green line which its implications will be later discussed – can be used to conduct measurements for single tone driven CMPs. Such CMPs can be modeled by employing the Input-Output formalism within the framework of the Hamiltonian approach [21]. In general, the Hamiltonian describing the whole system can be written as:

$$\mathcal{H} = \mathcal{H}_{\text{sys}} + \mathcal{H}_{\text{bath}} + \mathcal{H}_{\text{int}},\tag{1}$$

where $\mathcal{H}_{\text{sys}} = \hbar \omega_c a a^{\dagger} + \omega_m m m^{\dagger} + \hbar g_{\text{eff}} (a^{\dagger} m + m^{\dagger} a)$ which is also known as the Tavis-Cummings Hamiltonian for an N particle two-level system [21]. Here, \mathcal{H}_{sys} refers to the intracavity interactions such as the coupling between cavity photon and magnon where $a, a^{\dagger}, m, m^{\dagger}, g_{\text{eff}}$ denote the photon destruction and creation operators of the cavity photons, the magnons and the coupling strength, respectively. $\mathcal{H}_{\text{bath}}$ describes the external environment, i.e the bath; and \mathcal{H}_{int} is the interaction between the external field modes and the internal cavity photons. In the most simplistic case, we assume that there is no direct coupling of the intracavity system with the environment. Accordingly, we consider the Hermitian form of this Hamiltonian. We can then write equations of motion (EOM) for both the cavity photons (a, a^{\dagger}) and the magnons (m, m^{\dagger}) , which include damping and diffusion as:

$$\frac{dm}{dt} = -\frac{i}{\hbar}[m, \mathcal{H}_{\text{sys}}] - \kappa_m \cdot m, \quad \frac{da}{dt} = -\frac{i}{\hbar}[a, \mathcal{H}_{\text{sys}}] - \kappa_c \cdot a + \sqrt{2\kappa_e}b_{\text{in}}(t). \quad (2)$$

These expressions can then be combined in order to derive reflection $S_{11}(\omega)$ or transmission $S_{21}(\omega)$ parameters from Input-Output theory. However, these steps are familiar from Refs. [21, 24] for reflection and from Ref. [4] for transmission. Thus, we only summarize the basic assumptions in order to obtain the final equations. These are:

- 1. The magnons are not coupled to the external bath, but solely to the cavity photons.
- 2. The photons are coupled to the external bath which represents the input microwave field from the cavity port.
- 3. The following Input-Output relation between the signal entering and leaving the cavity resonator is utilised [21]: $b_{\text{out}}(\omega) + b_{\text{in}}(\omega) = \sqrt{2\kappa_{e,i}}a(\omega)$, where $b_{\text{out}}(\omega)$ and $b_{in}(\omega)$ denote the output and input from the microwave feedline to the cavity resonator port, respectively, and $a(\omega)$ is the internal cavity photon field.

Steering between Level Repulsion and Attraction: Beyond Single-Tone Driven Cavity Magnon-Polaritons7

The EOMs are then solved and, by means of a Fourier transformation, expressed as functions of the frequencies ω . These yield

$$S_{11}(\omega) = -1 + \frac{2\kappa_e}{i(\omega_c - \omega) + \kappa_c + \frac{g_{\text{eff}}^2}{i(\omega_m - \omega) + \kappa_m}}$$
(3)

for reflection. Here, κ_e are the losses due to the coupling to the microwave feedline into the resonator, κ_c the total (loaded) cavity resonator losses, ω_c is the resonance frequency of the cavity resonator, ω_m is the frequency of the magnons, and κ_m is the loss parameter for the magnons corresponding to the magnon linewidth.

3.2. Scattering parameters for two-tone driven CMPs

In order to harness the CMP for real applications, it is not sufficient to only obtain a strongly coupled cavity-magnon system, but instead, the coupling strength as a measure for coherent information exchange needs to be controlled. Among other ways to achieve a control of the coupling strength (c.f. [22, 24]), the approach of the introduction of a second microwave port to the system represents another possibility to obtain such a control [25, 28].

For this two-tone driven CMP, the above assumptions for the derivation of the S-parameters remain valid for the cavity port. However, the second port, which we call magnon port, ideally couples to the magnons only (this is the case shown in Fig. 1 when considering the effect of the green dotted line). As a result of the addition of the magnon port, the magnonic subsystem is now directly coupled to the external bath which perturbs the balanced gain and loss of the intracavity system in the presence of the cavity photon coupling without the magnon port [36]. Consequently, the intracavity system describing the cavity photon-magnon coupling is no longer a closed system but an open one.

Furthermore, the magnon port may differ in phase and amplitude which in addition with the direct coupling to the magnons results in a change of the expression for the scattering parameter $S_{11}(\omega)$ for a single tone driven CMP. This is discussed in the following.

As done previously for the simple hybrid system, our approach is based on an interaction Hamiltonian $\mathcal{H}_{\rm sys}$. However, in order to derive a new expression for $S_{11}(\omega)$, $H_{\rm sys}$ is modified. Now, we assume that the input from the microwave feedline, which couples to the cavity port, is given by $b_{\rm in,1}$. In the same way that the second port, which exhibits the relative phase shift, is given by $b_{\rm in,2}$. The resulting spectrum is recorded at the second port of the VNA which is configured for a transmission measurement. However, the signal there corresponds to the back-reflected signal from the cavity port, given by $b_{\rm out,1}$. The different roles and the labelling of both feedlines in our systems are sketched in Fig. 2. This schematics shows the cavity resonator with the inserted YIG sphere. Considering only $b_{\rm in,1}$, this input field corresponds to the classical cavity photon magnon-polariton experiments where both subsystems hybridize at resonance and form an avoided level crossing in the dispersion [4, 5]. The addition of the magnon

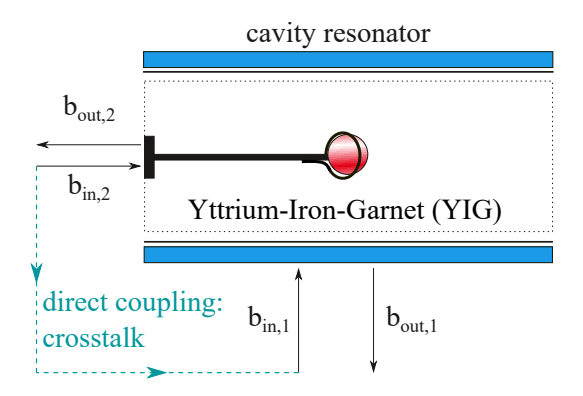


Fig. 2. Sketch of the different roles of the ports and thus their influence onto the coupled system. The cavity resonator is given as blue horizontal bars while the coupling loop of the second input is shown as a inductive coupler. The magnonic sample (red) is placed at the end. Here, $b_{\text{in},1}$ represents the microwave photon input field from the signal line directly exciting the cavity photons and it is the port where one measures the back-reflected signal and $b_{\text{in},2}$ is the input signal from the second input with the additional phase shifter inserted. The direct coupling between $b_{\text{in},2}$ to $b_{\text{in},1}$ is the what we refer to as crosstalk. The fields $b_{\text{out},1}$ and $b_{\text{out},2}$ are the outputs of the first and second input, respectively.

port (input $b_{\text{in},2}$) changes the system's properties drastically. The system's crosstalk is small for $\delta_0 \approx 1$ and is neglected in the following derivation. However, towards higher values of δ_0 , it's contribution increases and, hence, lowers the signal to noise ratio and has to be taken into account (c.f. Sec. 4.4).

As previously mentioned, only the microwave photons from the cavity port excite the cavity resonator photons. This excitation is expressed by the photon creation and destruction operators a and a^{\dagger} , respectively. Thus, the AC magnetic field originating from the magnon port serves solely as a direct input for the magnons.

The second driving field acts on the magnetisation and, hence, exerts an additional torque on the magnetisation [25]. If the phase and amplitude of this torque are chosen correctly, this torque compensates all dissipation channels including the coupling of the magnons to the cavity photons, and the avoided level crossing of the CMP coalesces. Level merging can be observed which also marks the transition to the regime of level attraction.

Therefore, the classical Tavis-Cummings Hamiltonian for a coupled system with N constituents is extended to a *driven* form. As the drive takes place via the coupling of the magnons to the cavity photons, the driving frequency, denoted by Ω , corresponds to the coupling strength g_{eff} modulated by the relative phase ϕ and amplitude δ_0 from the contribution of the second port. It is key that the second port is not just another microwave port of the cavity resonator but acts *indirectly* on the cavity resonator photons via the coupling of the magnons. Otherwise, the effect of a relative phase and amplitude would result in interference effects and not level merging of the CMP's dispersion.

Now, the system Hamiltonian $\mathcal{H}_{\rm sys}$ has to be modified to take into account this new contribution which results in an open system due to the direct coupling. The total number of particles is conserved and thus the first two terms respectively denote the total number of cavity photons $\hat{n}^{\rm photons} = a^{\dagger}a$ and magnons $\hat{n}^{\rm magnons} = m^{\dagger}m$ in the system. In contrast to Eq. 1, there are now two interaction terms in the system Hamiltonian. As previously, $H_{\rm int,1} = \hbar g_{\rm eff} \left(m^{\dagger}a + a^{\dagger}m \right)$ describes the interaction with coupling strength $g_{\rm eff}$ of the cavity resonator photons with the magnons and vice versa. The addition of a second interaction term $H_{\rm int,2} = \hbar g_{\rm eff} \delta_0 e^{i\phi} (a^{\dagger}m)$ considers the impact of the magnon port on the hybrid system via the coupling strength $g_{\rm eff}$.

As a consequence from our open system, we describe the two-tone driven CMP by a non-Hermitian Hamiltonian via:

$$\mathcal{H}_{\text{sys}} = \hbar \omega_c a^{\dagger} a + \hbar \omega_m m^{\dagger} m + \hbar g_{\text{eff}} \left(m^{\dagger} a + a^{\dagger} m \right) + \hbar \Omega \left(a^{\dagger} m \right),$$

where $\Omega = g_{\text{eff}} \delta_0 e^{i\phi}$. The last term is now interpreted as an additional drive of the cavity photons through the coupling to the magnons which are excited by magnon port.

The complex conjugated term of the last term is not included because this would correspond to the crosstalk, the direct interaction between the creation operator of the cavity resonator a^{\dagger} and the magnon lowering operator m. The addition of a second microwave input to the hybrid system leads to an additional torque exerted on the precessing magnetisation due to the induced change in the x- and z- components of the AC magnetic fields [c.f. Ref. [25]].

Depending on the magnitude and the orientation of this torque which is determined by δ_0 and ϕ , the system's dissipation can be compensated if $\delta_0 = 1$ or even result in an additional drive for $\delta_0 > 1$. In this picture, the coupling strength represents yet another dissipation channel which is then also compensated. Thus, tuning ϕ and δ_0 allows for a control of the coupling strength of the CMP in this specific system.

However, in order to include a control of the coupling strength via the additional torque which can compensate for the dissipation in the system, the above Hamiltonian needs to be non-Hermitian. Also, considering the 2×2 matrix by modeling the CMP, for instance, by two coupled harmonic oscillators where the off-diagonal elements representing the coupling terms [7], level merging is only possible if the product of the off-diagonal terms is negative. It cannot be a positive, real valued quantity because the interaction potential would be repulsive. Thus, this means that the sign of the off-diagonal product has to change.

Now, the equations of motion can be written down in Langevin form [21] as:

$$\begin{split} \frac{\partial m(t)}{\partial t} &= -i\omega_m m(t) - ig_{\text{eff}} a(t) - \kappa_m m(t) + \sqrt{2\kappa_{e,2}} b_{in,2}(t), \\ \frac{\partial a(t)}{\partial t} &= -i\omega_c a(t) - ig_{\text{eff}} (1 + \delta_0 e^{i\phi}) m(t) - \kappa_c a(t) + \sqrt{2\kappa_{e,1}} b_{in,1}(t), \end{split}$$

where ω_m denotes the magnon precession frequency, $g_{\rm eff}$ the effective coupling strength, $\kappa_{e,2}$ the coupling factor to the magnon port, ω_c the cavity photon frequency, κ_c the total resonator losses and $\kappa_{e,1}$ the coupling factor of the cavity port. After a Fourier transformation and employing the Input-Output relation for a system with one external port and a reflection measurement $b_{out,1}+b_{in,1}=\sqrt{2\kappa_{e,1}}a$ ([21]) the scattering parameter $S_{11}(\omega)$ can be expressed as:

$$S_{11}(\omega) = -1 + \frac{2\kappa_{e,1}}{-i(\omega - \omega_c) + \kappa_c + \frac{g_{\text{eff}}^2(1 + \delta_0 e^{i\phi})}{X}} - \frac{2ig_{\text{eff}}\delta_0 e^{i\phi} (1 + \delta_0 e^{i\phi}) \sqrt{\kappa_{e,1}\kappa_{e,2}}}{X\left(-i(\omega - \omega_c) + \kappa_c + \frac{g_{\text{eff}}^2(1 + \delta_0 e^{i\phi})}{X}\right)},$$

$$(4)$$

where $X=-i(\omega-\omega_m)+\kappa_m$. The first two terms can be mapped to Eq. (3) except a change in the term for the coupling strength from $g_{\rm eff}^2\to g_{\rm eff}^2(1+\delta_0e^{i\phi})$. In contrast, the term considering the coupling strength in the expression for Eq. (3) for the CMP driven with a single tone is purely real. This would be the full expression for the scattering parameter in the case of a single tone CMP. However, the additional input via the magnon's coupling to the cavity resonator photons has to be considered for the two-tone experiment. Hence, the third term considers this contribution. As the additional drive is mediated by the coupling to the cavity photons, it is proportional to $g_{\rm eff}$, i.e. the coupling in the limit $\delta_0 \to 0$ for different phases ϕ .

4. Results and Discussion

Having discussed the nature of the hybrid magnon-cavity system under various conditions, we now turn to the direct implications of two tones in a spectroscopic experiment.

4.1. Two-tone spectroscopy numerically analyzed

We start by looking at the characteristics of Eq. (4) regarding the coupling strength. One can see that g_{eff} is completely real for a "single-tone" driven CMP. However, in case of a second contribution, the previous expression for the coupling strength has to be rewritten as $g'(\delta_0, \phi)$ which reads as

$$g'(\delta_0, \phi) = g_{\text{eff}} \sqrt{1 + \delta_0 e^{i\phi}},\tag{5}$$

where g_{eff} corresponds now to the "single-tone" coupling strength, i.e. the coupling strength in the limit for $\delta_0 \to 0$.

For $\delta_0 = 1$ and $\phi = \pi$, the term in the square root vanishes and a complete merging of the frequency gap of the avoided level crossing in the dispersion spectrum is expected. Hence, this combination of relative phase and amplitude is what we describe as the onset of level merging. If the relative phase is kept constant at $\phi = \pi$ and δ_0 is further increased, the term $g'(\delta_0, \phi)$ describing the coupling between the cavity photons

and the magnons becomes purely imaginary denoting the regime of level attraction. In Fig. 3, the expected dependence of the complex coupling strength on δ_0 [(a) and (b)] and ϕ [(c) and (d)] is displayed for the real [(a) and (c)] and imaginary part [(b) and (d). The left column shows the real and imaginary part of the coupling strength as a function of the relative amplitude ratio δ_0 for three fixed values of the relative phase $(\phi \in 0, \pi/2, \pi)$. For $\phi = 0$, the coupling strength increases with δ_0 whilst remaining a real valued quantity. On the other hand, for $\phi = \pi$ the real part vanishes for $\delta_0 \geq 1$. Beyond this, the coupling strength is imaginary and increases for higher values of δ_0 . A relative amplitude ratio of $\delta_0 = 1$ constitutes the transition from level repulsion to level attraction via level merging at this specific δ_0 for $\phi = \pi$, because the sign of $g'(\delta_0, \phi)$ in Eq. (5) changes from positive to negative. Now, if we look back to the framework of two coupled harmonic oscillators, we can see that the repulsion between the antisymmetric and the symmetric mode is changed to an "attraction of the eigenvalues" of the coupled system. The relative phases of $\phi = 0$ and $\phi = \pi$ represent two special cases. Since either the imaginary $(\phi = 0)$ or the real part $(\phi = \pi)$ for $\delta_0 = 1$ are zero, these cases allow to attribute the real part of the coupling strength to level repulsion and the imaginary part to attraction, respectively. In this regard, for intermediate relative phase values, the coupling strength is comprised of both a repulsive and attractive contribution. The final shape of the spectrum then depends on whether for a specific relative phase the real or imaginary part is the dominant contribution. However, due to the non-zero contribution of the other, the dispersion spectra are slightly distorted by the coexistence of both repulsion and attraction.

In the case of $\phi = \pi/2$ [real part shown in Fig. 3(a) and imaginary part shown in Fig. 3(b)], the non-zero imaginary part acts to "damp" the increase of the coupling strength towards higher values of δ_0 . At this relative phase, both contributions are comparable in magnitude. Therefore, compared to the increase (decrease) for $\phi = 0$ and $\phi = \pi$ one should expect a strongly suppressed dependence of the coupling strength on δ_0 for $\phi = \pi/2$. In addition, the relative amplitude ratio can be kept fixed and the coupling strength studied as a function of the relative phase (c.f. Fig. 3 c.) and d.)). The dependence on ϕ is illustrated for three different values of δ_0 in Fig. 3 (c) for the real part and (d) for the imaginary part.

The real part of $g'(\delta_0, \phi)$ displays a periodic dependence on the relative phase in the interval -2π to 2π . For $\delta_0 < 1$ the coupling strength increases equally for $\phi = 0$ as and $\phi = \pi$ for the same value of δ_0 . Hence, the coupling is modulated, but for the regime of level merging the relative amplitude ratio δ_0 needs to be altered. For instance, if $\delta_0 \geq 1$ (green and red solid lines in Fig. 3 (c)), the coupling strength at $\phi = 0$ increases. However, at $\phi = \pi$, level merging sets in and the real part of $g'(\delta_0, \pi)$ goes to zero. At this point, the difference between the real part of $\delta_0 = 1$ and $\delta_0 = 2.63$ is negligible. This changes when the contribution from the imaginary part is also considered. For $\delta_0 < 1$, the coupling strength $g'(\delta_0 = \text{const}, \phi)$ is a continuous function for $\phi \in (-2\pi, 2\pi)$. However, at the transition to level merging, i.e $\delta_0 = 1$, it becomes discontinuous at $\phi = \pm \pi$. At this point, the value of the imaginary part of the coupling strength is no

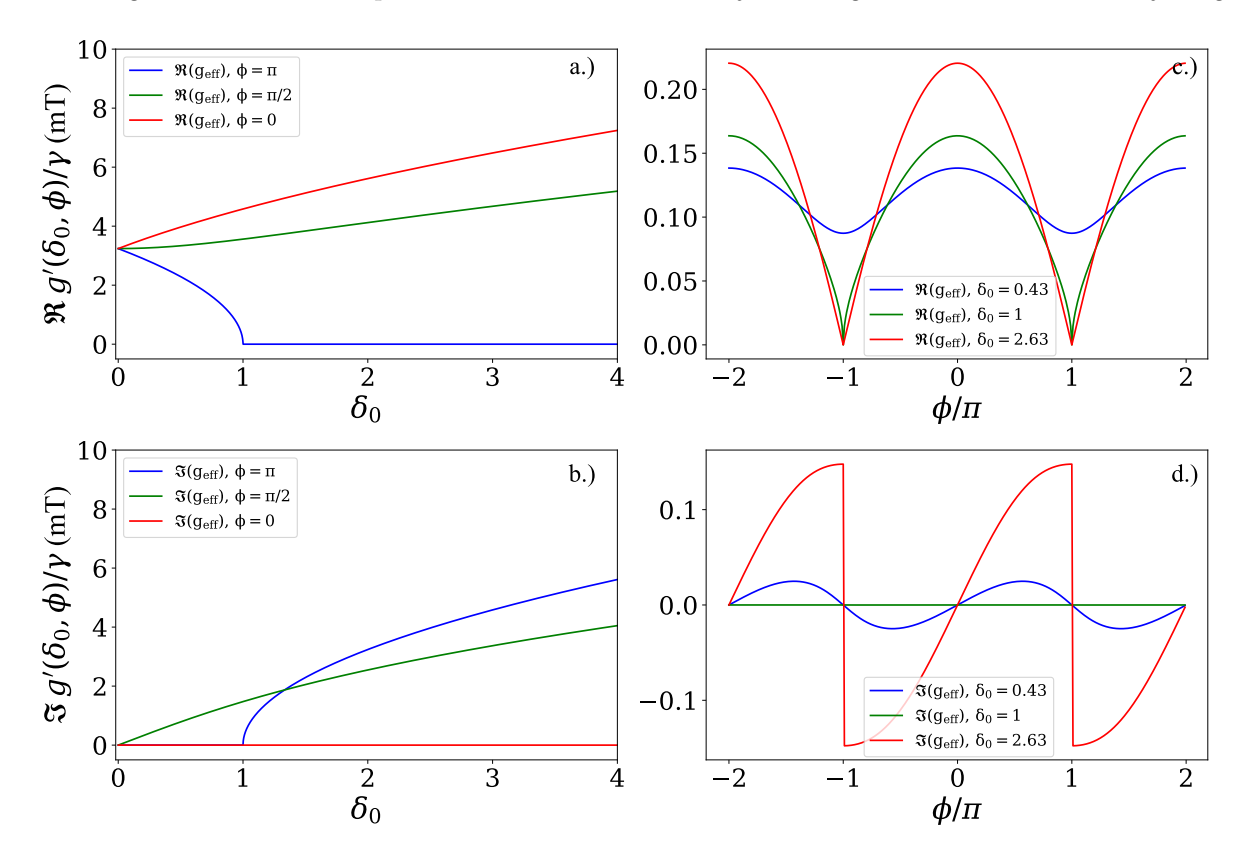


Fig. 3. Simulations of the dependence of the real and imaginary part of the complex coupling strength on the relative amplitude ratio δ_0 (a.) and b.)) and phase ϕ . (c.) and d.)). a.) Dependence of the real part of the coupling strength for three different values of the relative phase $(\phi \in (0, \pi/2, \pi))$. For $\phi = \pi$, the real part goes to zero for $\delta_0 \geq 1$ whilst for $\phi = 0$, the real part continues to increase. At the intermediate phase value of $\phi = \pi/2$, the coupling strength also increases but with a smaller gradient compared to $\phi = 0$. b.) Dependence of the imaginary part of the coupling strength for three phase values. Compared to a.) the imaginary part is always zero for $\phi = 0$, non-zero only when $\delta_0 \geq 1$ for $\phi = \pi$ and constantly increasing for all values of δ_0 for $\phi = \pi/2$. c.) The real part of the coupling strength as a function of $\phi \in (-2\pi, 2\pi)$ for three values of δ_0 below, at the onset of, and in the regime of level merging. The dependence is periodic for all δ_0 , with increasing maximums of the coupling strength for $\phi = 0$ and a sharp minimum at $\phi = \pi$ for $\delta_0 > 1$. Below $\delta_0 = 1$, the coupling is always suppressed. However, the slope for values close to π increases for higher δ_0 . d.) Imaginary part from the spectrum shown in c.). Above $\delta_0 = 1$, the plot becomes more and more antisymmetric in the sense of a "smooth" continuous transition at $\phi = 0$ and an increasing discontinuity, i.e sign change, at $\phi = \pi$.

longer uniquely defined. When the relative amplitude ratio is further increased, the discontinuity increases both in slope and magnitude. Just as in the previous description [(a) and (b)], the magnitude of the imaginary part is zero for all values of δ_0 when $\phi = 0$.

4.2. Two-tone cavity magnon-polariton spectroscopy

In our experiment for two-tone cavity magnon-polariton spectroscopy, the relative amplitude ratio δ_0 is defined as the ratio of the AC magnetic field from the magnon port and the cavity port, that is $\delta_0 = \frac{\mathbf{h}_{x,\text{magnon port}}^{AC}}{\mathbf{h}_{\text{cavity port}}^{AC}}$. Please note that in the experiment we are not able to directly measure the strength of the internal AC magnetic fields at the position of the sample. However, we can derive δ_0 from calculating an external amplitude ratio δ_{ext} which is defined as $\delta_{\text{ext}} = \frac{A_{\text{magnon port}}}{A_{\text{cavity port}}}$, where A denotes the amplitude of the microwave feedline at either port before it is coupled into the microwave resonator. The efficiency of the coupling, i.e. it's quality factor of the microwave signal into the resonator at either port can be determined from fitting a circle to the individual response from each port [37] and gives an additional factor to the external amplitude ratio. Then, δ_0 is calculated via $\delta_0 = \zeta \delta_{\text{ext}}$, where denotes an effective coupling factor for the coupling into the cavity [28].

The cavity port directly drives the cavity photons, i.e. the specific cavity mode. Typically, its amplitude is much higher than the initial amplitude contribution from the magnon port. As a result, in order to increase the value of δ_0 , the microwave feedline to the cavity port needs to be attenuated. Attenuating the cavity ports amplitude instead of amplifying the amplitude of the microwave signal which enters at the magnon port clearly prevents one from reaching a nonlinear regime for the CMP but also sets an intrinsic limit to our setup due to the presence of noise. The further the cavity port is attenuated, the lower the signal to noise ratio of the recorded data as we probe our system in reflection at the cavity port. Hence, the data analysis is more and more aggravated until clear statements on the specific nature of the signal are not possible any more. The subtle nature of crosstalk from magnon to cavity leading to an increasing signal, whereas the cavity reflection shows up as a decrease from the baselines signal renders the measured response very sensitive to the achievable cross-talk suppression. As for all microwave devices, reduction of unwanted signal leakage is far from trivial. As an example, a crosstalk of 1% corresponds to -20dB of applied power. A power ratio of -20dB corresponds to an amplitude ratio of 0.1. In this work, the relative signal amplitudes are described by δ_0 . That means for $\delta_0 > (0.1)^{-1} = 10$ (i.e. +20dB relative power to the magnon compared to the power at the cavity) the crosstalk signal from the magnon port dominates the cavity probing signal.

4.3. Interplay of attraction and repulsion for intermediate phases ($\delta_0 > 1$)

For the intermediate phases, we observe a coexistence of level merging and level attraction. Specifically, we show the coexistence for $\delta_0 = 1.31 \pm 0.22$ and $\phi = -\frac{3}{8}\pi$ in Fig. 4. Below resonance, the signature of an avoided crossing with a beginning opening of an anticrossing gap is visible. However, above resonance partially the triangular shape of the level attraction regime is also visible. Apart from showing the broad tunability of our two-tone driven approach to control the cavity magnon-polariton, the control of the relative contribution from level attraction (level merging) and repulsion (anticrossing)

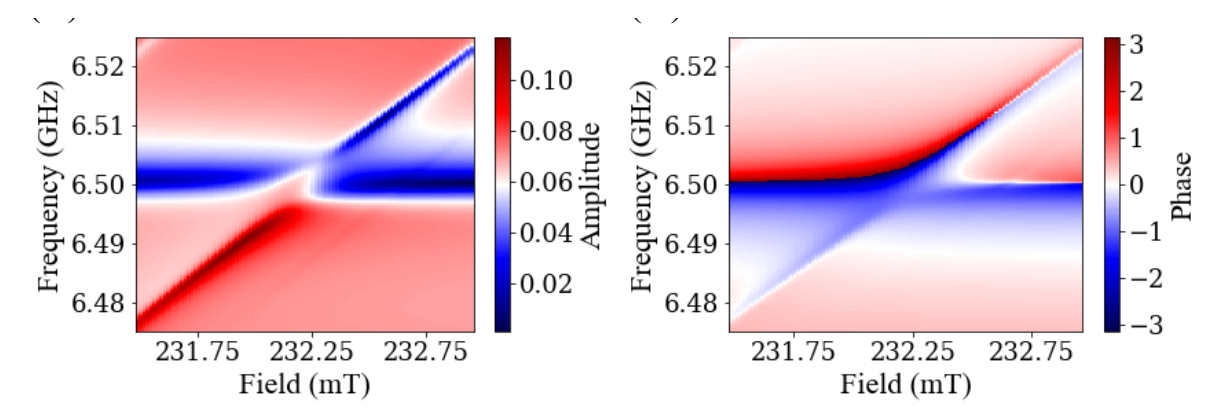


Fig. 4. Experimental data showing the "interaction" of level repulsion and attraction for $\delta_0 = 1.31 \pm 0.22$ and $\phi = -\frac{3}{8}\pi$ for amplitude (a.) and phase (b.). The counteracting repulsion and attraction at resonance lead to a partial extinction and partial enhancement of the signal. One can see both the characteristic features. First, the signal's curvature corresponding to the symmetric and antisymmetric mode of a "classical" avoided level crossing. Second, the existence of the triangular structure with the right apex more dominant than the left one.

might be interesting to generate intermediate states between maximum or minimum entanglement of cavity photon - magnon states and, hence, the transfer of information. For instance, the two-tone driven CMP can be transferred to the millikelyin temperature regime and these concepts tested in the single magnon regime as proposed in Ref. [38].

4.4. Towards high values of δ_0

As shown in Fig. 5 (a) for the amplitude and (b) for the phase response for $\phi = \pi$, for our system, the highest value was found to be $\delta_0 = 11.79 \pm 1.97$. The dashed lines serve as a guide for the eye and denote the level merging (black) and an anticrossing (yellow) spectrum. Whilst the first is the signal of interest, the latter is a result from a direct crosstalk, of our system which was suppressed as much as possible in the experiment but still non-zero [c.f. Ref.[28]]. Ideally, the AC field contribution from the magnon port does not couple to the cavity port. However, in case of a direct coupling, i.e. crosstalk, the magnon port serves as the input port and we measure an additional transmission signal at the cavity port due to that crosstalk. At the conditions for resonant coupling, the usual hybridization of a single-tone driven CMP sets in and is observed by an anticrossing. Thus, we measure the superposition of our level merging spectrum and the anticrossing due to crosstalk. An attenuation of the cavity port results in an increasing contribution of the magnon port which starts to dominate for $\delta_0 > 1$. Hence, for high values of δ_0 , the transmission signal due to crosstalk is higher in amplitude than the reflection signal of interest from level merging (c.f. Fig. 5 (a.)).

Consequently, for higher values of δ_0 where the exact value of δ_0 depends on the intrinsic amount of suppressing the crosstalk, it is not sufficient to only take the amplitude data into account to clearly identify the presence of level attraction of our system. Therefore,

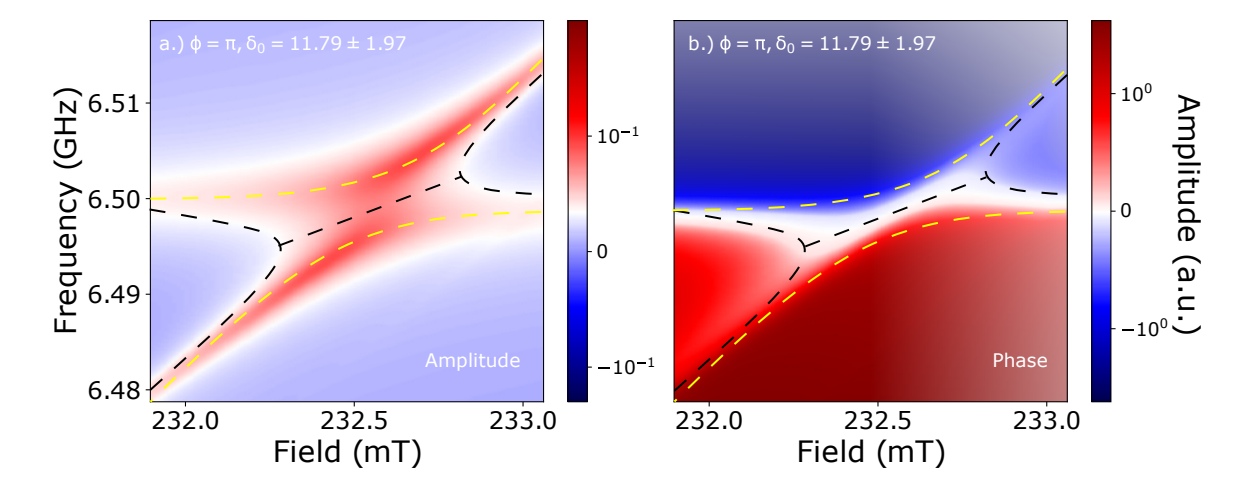


Fig. 5. Dispersion spectra of the amplitude (a.)) and phase (b.)) for $\phi = \pi$ and highest measured value of $\delta_0 = 11.79 \pm 1.97$ in a logarithmic scale. The spectra are a superposition of two signals, as indicated by the dashed lines, which serve as a guide for the eye. They are comprised of a level merging spectrum (black) with an additional avoided level crossing (yellow) at the same resonance frequency. The relative weight of the crosstalk measured in transmission at the cavity port increases towards higher δ_0 and has to be taken into account. Thus, for the complex-valued coupling strength, this avoided level crossing adds a parasitic real-valued contribution, which decreases the field distance between the apexes of the level merging signal and has to be considered in the calculation of $\Im(g'(\delta_0, \phi))$

the phase data has to be considered as well. As shown in Fig. 5 (b.)) and indicated again by the dashed black (level merging) and yellow (crosstalk anticrossing) it confirms the level merging signal for $\delta_0 = 11.79 \pm 1.97$.

5. Summary and outlook

In summary, we explained in detail one experimental approach to control the coupling strength by employing the relative phase and amplitude ratio δ_0 of a two-tone driven CMP. We numerically studied our new expression for-in the regime of level merging complex valued coupling strength. Furthermore, we experimentally demonstrated the coexistence of level attraction and level repulsion and the characteristics of the two-tone driven CMP in the limit of high δ_0 . Such coexistence not only demonstrates the broad tunability of our approach but also is highly interesting to realise some type of "superposition" states of the avoided level crossing and level merging regime where the amount of transmitted information flow can be exactly set. Since increasing δ_0 results in an enhancement of the relative weight of the crosstalk in the recorded signal, i.e. lowers the signal-to-noise ratio, we also show limitations of two-tone driven CMP coupling strength.

Moreover, we show that the system's Hamiltonian is non-Hermitian but depends on the phase and amplitude configurations and it can still result in real eigenvalues of the CMP.

This can be possible because, first, the introduction of a non-Hermitian term into the Hamiltonian denotes the possibility for an open system, i.e. dissipation is now included which is also referred to as approximate non-Hermiticity [39, 40]. For instance, this also describes radioactive decay or the introduction of dissipative systems in semiconductor physics. However, even for non-Hermitian systems, the spectra can be real if the system is \mathcal{PT} symmetric, i.e. is invariant under parity and time reversal transformations such that $[H, \mathcal{PT}] = 0$. \mathcal{PT} symmetric systems are studied in many different fields such as in quantum mechanics [41], optical microcavities [42] or magnetism and magnonics This symmetry also started to receive interest in cavity spintronics and for CMPs where the spectra and behaviour of \mathcal{PT} symmetric CMPs have recently been discussed [20, 44, 45]. As shown in Ref. [20], the \mathcal{PT} symmetric state is achieved by carefully engineering the losses from the cavity resonator and the magnons such that $\gamma_a = \kappa_c = \kappa_m$. Then, the coupling strength is tuned by moving the position of the YIG sphere in the cavity resonator. In case of $g_{\text{eff}} = \gamma_a$, the two separate eigenmodes of the coupled system coalesce to one point. This singularity in the eigenvalues represents the hallmark of a non-Hermitian system and this point is called an exceptional point (EP). What we show here, is the possibility to transition from avoided level crossing to level merging by tuning the relative orientation and amplitude of the additional torque added to the system. However, neither the cavity dissipation nor the magnon dissipation are directly accessed and tuned such as has been done in Ref. [22]. Rather, we change the relative contribution and orientation of the additional torque, which then enhances or compensates the intrinsic system's dissipation. The connection and incorporation of the experimental results from this two-tone driven system to the above discussion of \mathcal{PT} symmetry and singularities such as EPs requires further in-depth theoretical studies.

Finally, here we demonstrate control over the coupling regime without any direct changes of the experimental setup, thus improving measurement and analysis precision and being advantageous for real applications. Such control mechanism over the spin-photon interaction could pave the way for deliberately turning on and off the coherent exchange of information. That could enable future applications for data storage and information processing by the addition of a non-linear component such as a superconducting circuit to the spin-photon system. Furthermore, it could be used for universal computing applications, where the dynamic control of the CMP on demand and within nanoseconds is an indispensable requirement. By performing fast manipulations of the polariton modes with two independent but coherent pulses to the cavity and magnon system [46] building blocks for a quantum internet can be realized, and thus, pave the way for further magnon-based quantum computing research.

Acknowledgement

We acknowledge valuable discussions with Dmytro Bozhko, Tim Wolz, Can-Ming Hu, Bimu Yao, Vahram L. Grigoryan, Ka Shen, and Ke Xia. This work is supported by the European Research Council (ERC) under the Grant Agreement 648011 and the DFG

REFERENCES 17

through SFB TRR 173/Spin+X. R. Macêdo acknowledges the support of the Leverhulme Trust.

References

- [1] Soykal Ö O and Flatté M E 2010 Physical Review Letters 104 077202
- [2] Huebl H, Zollitsch C W, Lotze J, Hocke F, Greifenstein M, Marx A, Gross R and Goennenwein S T B 2013 *Physical Review Letters* **111** 127003
- [3] M Goryachev, W G Farr, D L Creedon, Y Fan, M Kostylev, and M E Tobar 2014 *Phys. Rev. Appl.* **2** 054002
- [4] Y Tabuchi, , S Ishino, T Ishikawa, R Yamazaki, K Usami, and Y Nakamura 2014 Phys. Rev. Lett. 113 083603
- [5] X Zhang, C-L Zou, L Jiang, and H X Tang 2014 Phys. Rev. Lett. 113 156401
- [6] Zhang X, Zou C L, Zhu N, Marquardt F, Jiang L and Tang H X 2015 Nat. Commun.
 6 8914
- [7] Harder M and Hu C M 2018 Cavity spintronics: An early review of recent progress in the study of magnon–photon level repulsion *Solid State Physics* (Elsevier) pp 47–121
- [8] Lachance-Quirion D, Tabuchi Y, Gloppe A, Usami K and Nakamura Y 2019 Applied Physics Express 12 070101
- [9] Pfirrmann M, Boventer I, Schneider A, Wolz T, Kläui M, Ustinov A V and Weides M 2019 arXiv (Preprint http://arxiv.org/abs/1903.03981v1)
- [10] Sharma S, Blanter Y M and Bauer G E W 2017 Physical Review B 96 094412
- [11] Kusminskiy S V, Tang H X and Marquardt F 2016 Physical Review A 94 033821
- [12] Graf J, Pfeifer H, Marquardt F and Kusminskiy S V 2018 Physical Review B 98 241406
- [13] Zhang X, Zou C L, Jiang L and Tang H X 2016 Science Advances 2 e1501286
- [14] Hisatomi R, Osada A, Tabuchi Y, Ishikawa T, Noguchi A, Yamazaki R, Usami K and Nakamura Y 2016 Physical Review B 93 174427
- [15] Y Tabuchi, S Ishino, A Noguchi, T Ishikawa, R Yamazaki, K Usami, Y Nakamura 2015 Science 349 405–408
- [16] Haigh J, Nunnenkamp A, Ramsay A and Ferguson A 2016 Physical Review Letters 117 133602
- [17] Yao B, Gui Y S, Rao J W, Kaur S, Chen X S, Lu W, Xiao Y, Guo H, Marzlin K P and Hu C M 2017 Nat. Commun. 8 1437
- [18] Rao J W, Kaur S, Yao B M, Edwards E R J, Zhao Y T, Fan X, Xue D, Silva T J, Gui Y S and Hu C M 2019 Nature Communications 10 2934
- [19] Wang Y P, Zhang G Q, Xu D, Li T F, Zhu S Y, Tsai J S and You J Q 2019 (Preprint http://arxiv.org/abs/1903.12498v1)

REFERENCES 18

[20] Zhang D, Luo X Q, Wang Y P, Li T F and You J Q 2017 Nat. Commun. 8 1368

- [21] D F Walls and G F Milburn 2008 Quantum Optics (Springer-Verlag GmbH)
- [22] N R Bernier, L D Tóth, A K Feofanov, and T J Kippenberg 2018 Phys. Rev. A 98 023841
- [23] Grigoryan V L and Xia K 2019 Physical Review B 100 014415
- [24] Harder M, Yang Y, Yao B, Yu C, Rao J, Gui Y, Stamps R and Hu C M 2018 Phys. Rev. Lett. 121 137203
- [25] Grigoryan V L, Shen K and Xia K 2018 Phys. Rev. B 98 024406
- [26] Proskurin I, Macêdo R and Stamps R L (Preprint http://arxiv.org/abs/1904. 11570v1)
- [27] Bhoi B, Kim B, Jang S H, Kim J, Yang J, Cho Y J and Kim S K 2019 *Physical Review B* **99** 134426
- [28] Boventer I, Dörflinger C, Wolz T, Macêdo R, Lebrun R, Kläui M and Weides M (*Preprint* http://arxiv.org/abs/1904.00393v1)
- [29] Alexander G Gurevich G A M 2000 Magnetization Oscillations and Waves (CRC PR INC) ISBN 0849394600 URL https://www.ebook.de/de/product/4297668/alexander_g_gurevich_gennadii_a_melkov_magnetization_oscillations_and_waves.html
- [30] M Harder, L Bai, C Match, and C-M Hu 2016 Sci. China Phys. Mech. 59 117511
- [31] Y Cao, P Yan, H Huebl, S T B Goennenwein, and G E W Bauer 2015 *Phys. Rev.* B 91 094423
- [32] L Bai, M Harder, Y P Chen, X Fan, J Q Xiao, and C-M Hu 2015 *Phys. Rev. Lett.* **114** 227201
- [33] Sebastian T, Schultheiss K, Obry B, Hillebrands B and Schultheiss H 2015 Frontiers in Physics 3
- [34] Boventer I, Pfirrmann M, Krause J, Schön Y, Kläui M and Weides M 2018 Phys. Rev. B 97 184420
- [35] Ferrisphere Inc 15 Falcon Rd. Flanders, NJ 07836. United States
- [36] Bender C M 2018 Basics of PTsymmetry PT Symmetry (WORLD SCIENTIFIC (EUROPE)) pp 3–38
- [37] S Probst, F B Song, P A Bushev, A V Ustinov, and M Weides 2015 Rev. Sci. Instr. 86
- [38] Yuan H Y, Yan P, Zheng S, He Q Y, Xia K and Yung M H (*Preprint* http://arxiv.org/abs/1905.11117v1)
- [39] Bender C M, Brody D C and Jones H F 2002 Physical Review Letters 89 270401
- [40] Bender C M, Dorey P E, Dunning C, Fring A, Hook D W, Jones H F, Kuzhel S, Lévai G and Tateo R 2018 *PT Symmetry* (WORLD SCIENTIFIC (EUROPE))
- [41] Bender C M and Boettcher S 1998 Physical Review Letters 80 5243–5246

REFERENCES 19

[42] Wen J, Jiang X, Jiang L and Xiao M 2018 Journal of Physics B: Atomic, Molecular and Optical Physics 51 222001

- [43] Galda A and Vinokur V M 2018 Physical Review B 97 201411
- [44] Harder M, Bai L, Hyde P and Hu C M 2017 Physical Review B 95 214411
- [45] Cao Y and Yan P 2019 Physical Review B 99 214415
- [46] Wolz T, Stehli A, Schneider A, Boventer I, Macêdo R, Ustinov A V, Kläui M and Weides M (*Preprint* http://arxiv.org/abs/1906.08103v2)